Wg and Wnt4 provide long-range directional input to planar cell polarity orientation in *Drosophila*

Jun Wu[1], **Angel-Carlos Roman**[2], **Jose Maria Carvajal-Gonzalez**[1], and **Marek Mlodzik**[1,*]

[1]Dept. of Developmental & Regenerative Biology, Graduate School of Biomedical Sciences, Icahn School of Medicine at Mount Sinai One Gustave L. Levy Place New York, NY 10029 phone: 1-212-241 4272

[2]Instituto Cajal, CSIC Av. Doctor Arce 37 28002 - Madrid (Spain)

Abstract

Planar cell polarity (PCP) is cellular polarity within the plane of an epithelial tissue or organ. PCP is established through interactions of the core Frizzled(Fz)/PCP factors and although their molecular interactions are beginning to be understood, the upstream input providing directional bias/polarity axis remains unknown. Among core PCP genes, Fz is unique as it regulates PCP both cell-autonomously and non-autonomously, with the extra-cellular domain of Fz acting as a ligand for Van-Gogh (Vang). We demonstrate in *Drosophila* wings that Wg and dWnt4 provide instructive regulatory input for PCP axis determination, establishing polarity axes along their graded distribution and perpendicular to their expression domain borders. Loss-of-function studies reveal that Wg/dWnt4 act redundantly in PCP determination. They affect PCP by modulating the intercellular interaction between Fz and Vang, which is thought to be a key step in setting up initial polarity, thus providing directionality to the PCP process.

Planar cell polarity (PCP) is defined as cellular polarity within the plane of an epithelium and associated with many tissues and organs[1–7]. The conserved process of PCP establishment has been studied extensively in *Drosophila*, defining a core group of conserved factors around the Frizzled (Fz) protein, including *fz* itself, *Van Gogh* (*Vang*, a.k.a *strabismus/stbm*), *flamingo* (*fmi*, a.k.a *starry night/stan*) and others[1–8]. At early developmental stages, PCP core proteins interact with unknown upstream regulatory molecules as well as each other, to initiate and maintain their polarized localization, the first visible PCP feature. Within the Fz–core group, Fz is unique as it regulates PCP both cell-autonomously and non-autonomously[9, 10], with the extra-cellular domain of Fz acting as a ligand for Van-Gogh (Vang)[11]. Intercellular interactions between Fmi-Fmi and Fz-Vang are essential in specifying and propagating PCP direction[11,12]. Fmi-Fmi interactions form homophyllic bridges across cell membranes and facilitate intercellular Fz-Vang interactions, as Fmi physically interacts with both Fz and Vang[13–15], these factors also provide

*Correspondence should be addressed to MM: marek.mlodzik@mssm.edu.

asymmetry to Fmi-Fmi interactions as Fmi/Fz-Fmi/Vang intercellular bridges[11,16,17]. Dishevelled, Prickle, and Diego are intracellular core Fz/PCP-molecules involved in feedback loops to enhance and stabilize an initial polarity bias and activate downstream effectors within the cell[18,19]. A second molecular system regulating PCP acts in parallel and is centered on the protocadherins *fat* and *dachsous* and their regulator *four-jointed* (*fj*)[20–23]. Although intracellular molecular events in Fz/PCP signaling are beginning to be understood[1–4], the mechanism(s) of long-range PCP orientation across whole tissues remain elusive. It has been proposed that graded Fz activity directs PCP orientation towards lower Fz activity[9], supported by manipulations of Fz levels[9,11,24]. Endogenous Fz protein is, however, evenly expressed in all tissues tested, and therefore Fz "activity" must be regulated post-translationally in a graded manner, the mechanism(s) of which are unknown.

Wnt proteins, mainly Wnt5a and Wnt11, are involved in vertebrate PCP establishment, but their mechanistic input to PCP regulation remains unclear[25–30]. Although a Wnt5a gradient can generate a graded Vangl2 phosphorylation during digit formation in mouse limbs, with this also depending indirectly on Ror2 activity[29], it is not resolved whether vertebrate Wnts provide a permissive or instructive input directly to regulate Fz/Fmi PCP-interactions. PCP in *Drosophila* wing can be affected by morphogenetic organizers[31], with the dorso-ventral organizer set up by Notch and Wg-signaling and the antero-posterior organizer via Hedgehog and Dpp-signaling in 3rd instar larval discs. As the organizers control wing patterning, size and proliferation and the axes within the wing generally, their positional information could provide the earliest cues for PCP orientation[31]. Consistent with our data (see below), PCP orientation of the vast majority of cells in the 3rd instar larval wing pouch correlates with the dorso/ventral-organizer[31]. Canonical Wg/β-catenin signaling serves a major patterning role at these early stages, and thus it is difficult to distinguish (at that stage) whether a Wg effect on PCP is through canonical Wg-signaling or directly via Fz/PCP signaling. Moreover, in *Drosophila* the question of Wg/Wnt-Fz involvement in PCP establishment is not resolved and conflicting data exists[13,32,33].

Wnt4 and Wg misexpression reorients PCP

As the extra-cellular domain of Fz, mainly the Wnt binding CRD, is necessary and sufficient for the non-autonomous function of Fz[11], we revisited these issues and asked systematically, whether and how Wnts might function in *Drosophila* PCP generation. Wg, dWnt4 and Wnt6 are all expressed in identical patterns during *Drosophila* imaginal disc development[34–36]. Their expression domain at the wing margin is near perpendicular to the initial PCP axes, radial towards the wing margin (Fig. S1a; also[31,37,38]), and also in the eye PCP-specification occurs at the stage when R3/R4 are aligned perpendicular to the Wnt expression domains at the poles of the eye field (Fig. S1a', ref[39]), suggesting that they could provide directional cues. In adult wings, PCP orientation is still pointing towards wing margin in areas near the margin (Fig. 1a–c). Planar polarization in the wing progressively strengthens during early pupal stages[37], suggesting that PCP requires also later input for its strengthening, refinement and maintenance. The wing is an ideal model for these analyses, being a simple epithelial tissue and, importantly, canonical Wg-Fz/β-catenin signaling requirements are much reduced at pupal stages and (at least partially) temporally separable from Fz/PCP-establishment[34,40,41].

To bypass global patterning roles of Wnts (especially Wg) via canonical Arm/β-catenin signaling, which precludes PCP analyses at pupal stages, we examined the role of Wnts in PCP signaling during early pupal development, when most other wing patterning events are completed. At early pupal stages (<17h APF), cellular PCP orientation is radial and polarity directed towards the margin[37] (Fig. 1d-d"), where Wg and other Wnts are expressed throughout wing development[42,43] (Fig. 1e), consistent with a hypothesis that Wnts could provide directional long-range control to Fz/PCP-signaling. To circumvent potential redundancy associated with overlapping expression domains of several Wnts (see above), we first used gain-of-function (GOF) approaches by misexpressing each *Drosophila* Wnt in developing wings (using the Gal4/UAS system with either clonal or regional [*dppGal4*] expression[44]). Whereas most Wnts did not display PCP effects (all *wnt*-genes in the genome were tested), expression of dWnt4 and Wg caused striking and classical PCP defects, affecting cellular (wing hair) orientation of neighboring wild-type cells (Fig. 2a–c, Fig. 3). These data are consistent with earlier reports, suggesting that misexpression of Wnt4 can cause PCP phenotypes in the wing[32,45], and also with suggestions that Wg overexpression can affect PCP[31]. Strikingly, the phenotypes of Wg and dWnt4 misexpression were similar to non-autonomous polarity defects associated with *fz⁻* clones (surrounding wild-type cells orienting towards mutant area[9,24]) and opposite to Fz GOF defects (wild-type cells orienting away from Fz-overexpression regions[9,11,24]).

To establish that these GOF phenotypes are mediated by Fz/PCP signaling, and not by potential effects of the canonical Wnt/β-catenin pathway, we induced Wnt4-expressing clones in *fz⁻* null mutant wings (the entire animal lacks *fz*, but can signal canonically via the dFz2 receptor). Consistent with a direct effect of Wnt4 via Fz/PCP signaling, the cellular reorientation of cells neighboring Wnt4-expressing clones was eliminated in *fz⁻* backgrounds (Fig. 2d) and cellular orientation was basically identical to the patterns in *fz⁻* mutant wings alone (Figure 2d–e; 8/8 Wnt4-expressing clones caused no change to *fz⁻* mutant wing cell orientations; also Suppl. Fig. S1e-e'). Further confirming that the PCP effects were not mediated through canonical Wg-Wnt/β-catenin signaling, Wnt4-expressing clones did not affect expression of any canonical Wnt/Wg-targets[46–48] in larval or pupal wings (e.g. *Dll* and *fj-lacZ*, Fig. S1b–d). Taken together, the genetic epistasis data (Fig. 2d–e and Suppl. Fig. S1e-e') and the expression studies (Suppl. Fig. S1b–d) indicate that the Wnt GOF PCP phenotypes are mediated through Fz/PCP-signaling and that Fz acts downstream of Wnts in this context.

Wnt misexpression alters Fz/PCP factor localization

If Wnts regulate Fz/PCP-activity, their misexpression should not only affect wing hair orientation, but also alter core PCP factor polarization and hence PCP axis orientation at critical early stages of PCP establishment. To examine this functionally, we used Wnt4 clonal expression (which has no effect on canonical Wnt-signaling, see above) and analyzed pupal wings throughout PCP patterning. At early stages (prepupae-16h APF), when PCP axes are radial[37], Wnt4 clones strikingly reorient core PCP factor polarity (determined via Fmi staining) to a near 90° angle relative to clonal borders (Fig. 4a-a", c, d-d", compare to wild type, Fig. 4b-b'; see figure legend for statistical analyses). Similarly, at later stages (~30–32h APF) when PCP orientation has been realigned to the proximo-distal axis (and

actin prehairs have started to form) Wnt4-expressing clones continue to reorient surrounding cells towards clonal borders (Fig. 2c-c' and 3b-b", d; see legend for statistical evaluations). Of note, the near 90° reorientation of cells (relative to clonal borders, Fig. 4a,c,d) is mirrored by border cells on the inside of clonal margins, an effect likely mediated by intercellular feedback loops[18,19]. Also, Wnt4-expressing cells inside clones are less polarized compared to surrounding non-expressing cells as measured by their nematic order (length of polarity lines in Fig. 3b," and 4a,d; see figure legend for statistics), the exception again being border cells (marked by orange dots in Fig. 4a"), which are polarized relative to their outside neighbors (blue dots in Fig. 4a"; see legend for details). Overall, the frequency (72%) and effects seen with the Wnt4 misexpression clones are very comparable to *fz*- null clones [around 80% frequency in our hands], consistent with the notion that the Wnt effect and Fz/PCP mediated orientation are linked. Taken together, our data indicate that (1) Wnt4 and Wg can reorient cell polarity towards their expression domain (similar to *fz*- clones), and (2) that this polarity depends on a Wnt expression border (and possibly graded Wnt distribution), rather than high uniform Wnt levels (as demonstrated by the reduction of nematic order/polarity strength inside Wnt-expressing clones; Fig. 3 and 4 legends). Both observations indicate that Wnts serve an instructive role in establishing a PCP orientation axis. Taken together, we hypothesize that dWnt4 and Wg instruct the direction of Fz/PCP function and based on the opposing phenotypes of Fz and Wg/dWnt4-expressing clones, possibly by inhibition of the non-autonomous Fz function in PCP establishment.

wg and *dWnt4* are necessary for PCP establishment

To determine whether Wnt4 and/or Wg are also necessary for Fz/PCP axis orientation, we examined loss-of-function (LOF) phenotypes. As Wg and dWnt4 are expressed in an identical pattern and both display comparable GOF PCP effects (see above), the lack of a LOF phenotype in *dWnt4^EMS23* genetic null mutants (Fig. 5d; *dWnt4* mutants also do not show PCP phenotypes in the eye[33]) could be due to redundancy with *wg*. LOF *wg* studies reveal strong canonical Wnt/β-catenin signaling defects throughout development, precluding simple PCP analyses. To limit the early Wg-requirements, we used a temperature sensitive allele, *wg^IL114*, and removed Wg function only later. *wg^CX3* is a hypomorphic allele with reduction in Wg expression at the margin (Suppl. Fig. S2), accompanied by genetic wing margin defects[49]. In *wg^CX3/IL114* wings that were shifted to the non-permissive temperature in early prepupae (see Methods), most wings displayed wild-type PCP features (Fig. 5a-a"). To further reduce Wnt function and to address potential redundancy between Wg and dWnt4, we examined double mutant wings for *wnt4^−/−*, *wg^CX3/IL114* (completely removing *wnt4* and partially *wg*, shifted as above, see Methods; importantly, the stronger *wnt4^− wg^IL114* double homozygous animals were lethal prior to 3rd instar stages even at the permissive temperature, and hence the need for the hypomorphic *wg^CX3/ts* combination). Strikingly, wings from such animals displayed robust PCP defects, both in pupal wings (Fig. 5a–c'; note that such animals did not eclose and thus were analyzed at pupal stages with molecular markers) as well as at early stages (prepupa -16h APF; Fig. 6). PCP defects were not only evidenced by misoriented cellular hairs (actin staining in Fig. 5b, green; see also Suppl. Fig. S3e–f for orientation defects in rare adult escapers), but importantly also by defects in the early pupal polarization axes of core PCP factors (detected via Fmi staining,

Fig. 5a–c' and Fig. 6). Importantly, these results suggest a requirement of *wg*, *dWnt4* at the critical, early stages of PCP axis definition. Whereas wild-type cells polarize towards the wing margin and display strong polarization (measured by nematic order, length of yellow lines in individual cells in Fig. 6a",b",c', longer lines correspond to stronger polarization), the *wg*, *dWnt4* double mutant wings lacked coordinated cellular orientation, mutant cells showed a wide distribution of polarity angles (Fig.6b–c') and displayed reduced overall polarization (evident in nematic order levels reduced to 60% [$p=10^{-26}$] in the double mutant; see Fig. 6 legend for details). Interestingly, cells near the wing margin were oriented parallel to the margin in the double mutant background (e.g. pink "nematic order" lines in Fig. 6b"), which is consistent with the proposal that cells in/at the margin respond to cues from the antero-posterior organizer (in 3rd instar stages)[31] and are less polarized in wild-type at early pupal stages[37] (pink "nematic order" lines in cells in Fig. 6a"c and ref[37]). Together with the GOF data, these results indicate that Wnts are not only instructive but also necessary for *Drosophila* PCP axis establishment.

Wg/Wnt4 modulate intercellular Fz-Vang interaction

Fz and Vang/Stbm interact physically with each other through their extracellular domains between cell membranes of neighboring cells in culture and *in vitro*[11,15] and thus presumably also *in vivo*. This interaction is thought to serve as a sensing mechanism of Fz levels/activity, and thus a determinant of PCP direction[11]. Since Wnts bind Fz CRDs[50–52] and affect PCP orientation (Figs. 2–6), we hypothesized that a Wnt-Fz association could modulate the Fz-Vang interaction, thus creating the "sought-after" Fz-PCP activity gradient; it would be oriented along a Wnt-gradient emanating from the source of Wg/Wnt4, as suggested by our GOF and LOF studies. We first tested whether Wg and/or Wnt4 can interfere with the Fz-Vang interaction in a cell-based recruitment assay[15]. This assay is well suited, as it directly detects an intercellular Fz-Vang interaction across cell membranes of neighboring cells, similar to the context of PCP axis specification. Fz-expressing S2+R cells recruit Vang in neighboring cells to the membrane via cell-cell contact (Fig. 7a–b). As S2+R cells are normally not adhesive and only a very small fraction of Fz and Vang expressing cells touch each other, we aided adhesion by co-transfecting with *Drosophila* E-cadherin (E-cad; to promote cell-cell contacts via homophilic E-cad interactions) with either Fz or Vang. Fz/E-cad expressing cells recruit Vang to the membrane at cell contacts with Vang/E-cad expressing cells (Fig. 7a-a"). To test whether Wg or Wnt4 can affect this Fz-Vang recruitment, we co-transfected the Fz/E-cad cells with Wg. Strikingly, co-transfection of Wg, reduced Vang recruitment in a specific and dosage dependent manner (Fig. 7c–e; see also Suppl. Fig. S4a; quantification reflects Vang membrane localization in individual cells in contact with Fz expressing cells; control transfections included non-related secreted ligands, e.g. the Jak/STAT-signaling ligand Upd; Fig. 7c-c'"). To confirm that this is a non-autonomous (extracellular) effect, we tested conditioned media (CM) containing secreted Wg or Wnt4 (and again Upd as control) in the same assay. The Fz-Vang recruitment was similarly decreased in Wg-CM and Wnt4-CM conditions (Fig. 7f; also Suppl. Fig. S4b–d"), indicating that extracellular Wg and Wnt4 are interfering with intercellular Fz-Vang interactions. These data confirm that Wg/Wnt4 can act as dosage dependent modulators of the Fz-Vang interaction during PCP establishment. To confirm these effects on Fz activity *in*

vivo, we tested whether the Fz GOF PCP phenotype can be modified by Wnt4 co-expression. Strikingly, co-expression of Wnt4 with Fz (in the *dpp-Gal4* domain[11]) markedly reduced the non-autonomous effects of Fz overexpression on cells outside the *dpp* domain (Fig. 8a–c; and Suppl. Fig. S5). These data are consistent with a previous report showing that Wnt4 can antagonize Fz overexpressing phenotypes[32] (although a different Fz phenotype was assessed there[32]). In summary, Wnt4/Wg can modulate the Fz-Vang interaction, possibly by antagonizing Fz signaling activity to neighboring cells.

Discussion

Our data indicate that Wg/dWnt4 regulate the establishment of Fz/PCP axes by modulating the Fz-Vang intercellular interactions in a graded, dosage dependent manner. Consequently they might generate different levels of Fz-Vang interactions across a Wg/dWnt4 gradient experienced by cells (see model in Fig. 8d). This process is reiterated across the tissue and the directionality of Fz-Vang binding is subsequently reinforced by intracellular core PCP factor interactions[18, 19]. Our data are consistent with a model in which Wg/dWnt4 generate a Fz-"activity" gradient by modulating its capacity to bind to Vang, consistent with proposals of Fz-"activity" gradient models[9,39]. Accordingly, PCP axes are orientated towards the Wg/dWnt4 source, which is evident in (at least) the wing and eye. The early wing PCP axis (late larval to early pupal stages) correlates well with Wg/dWnt4 margin expression[31,37] and, similarly, in the eye polarity is oriented in the dorsal-ventral axis towards the poles where Wg/Wnt4 are expressed (illustrated in Suppl. Fig. S1a-a'). This model relying on a Fz-Vang interaction is also compatible with the addition of Fmi to this scenario, with intercellular (homophillic) Fmi-Fmi interactions also being required for PCP specification[12]. As Fmi forms complexes with both Fz and Vang, the full complement of intercellular interactions includes Fz/Fmi-Fmi/Vang complexes[13–15], and these interactions would also be modulated by Wnt binding to Fz, either directly as proposed in our model or possibly by modulating the Fmi-Fmi interactions by having Fmi associated with Fz that is bound to different levels of Wg/Wnt4. *In vivo*, Fmi helps to enrich both Fz and Vang to the sub-apical junctional region, and Fmi-Fmi interactions bring Fz and Vang to close molecular proximity. Intercellular Fmi-Fmi interactions are strong, as Fmi expressing S2 cells form cell-aggregates through homophilic Fmi interactions[12]. The interaction between Fz and Vang is weaker and cell-cell contacts between the two cell groups are infrequent[15]. It was suggested that PCP signal sensing complexes include both Fmi and Fz on one cell interacting with Fmi/Vang at the surface of a neighboring cell. Within these complexes, Fz is required for sending a polarity signal[11,17], whereas Fmi and Vang are involved in its reception[11,17], consistent with our data and model. Although it has been suggested that Fmi is capable of sensing Fz/Fmi signals in the absence of Vang[17], the "Fz-sensing" capability of cells with Fmi alone (lacking Vang) is much weaker than that of cells with Vang[17]. It will be interesting to determine if there are additional PCP regulators directly involved in modifying Fmi-Fmi interactions.

How does our data relate to previous models and why was the Wg/Wnt4 requirement not observed before? Previous work attempted to address the role of the wing margin on PCP by examining either mutants affecting wing margin cells without eliminating *wg/Wnt* expression[53] or in clones[13]. Although cellular hairs near the site of wing margin loss pointed towards remaining wing margin areas, the effect was considered weak. We also examined

potential effects of Wnt LOF clones of *Df(2L)NL*, lacking *wnt4*, *wg*, *wnt6* and *wnt10*. In contrast to the global reduction of Wg/Wnt4 through the temperature sensitive *wg*-allele, such clones do cause only mild PCP perturbations (Figure S3a–c). There are several reasons why clonal loss of Wnt expression in the margin only mildly affect PCP orientation: (1) Cells can respond to Wnts from several sources/cells from remaining Wnt-expressing wing margin regions (illustrated in Fig. S3a'); (2) polarization strengths (measured by nematic order) in the first few rows of cells near the margin are much weaker than cells further way (at 14–17h APF ref[37]) and weak PCP reorientation in cells neighboring wing margin clones could thus reflect the initial weak polarization in these cells; and (3) PCP orientation changes from its initial radial polarity towards the proximo-distal polarity during hinge contraction morphogenesis and associated cell flow[37], likely leading to significant corrections of subtle defects near the margin. Similarly, PCP orientation in cells near the margin is only very weak early (at 14–16h APF[37]), likely because cells close to the Wnt-producing cells are exposed to saturated Wnt-levels (and not a Wnt–gradient) or the presence of other organizers (directing polarity parallel to the margin[31]) weakens the effect of Wnts. PCP in these cells gets established/corrected through more local interactions during the feedback loops among neighboring cells.

To determine the direct role of Wg/Wnts on Fz/PCP signaling, we examined it at pupal stages as the patterning role of canonical Wg-signaling is much reduced then and PCP still correlates well with Wg/Wnt4 expression (ref[37] and this study). Importantly, Wnt4 does not affect expression of patterning genes via canonical signaling at larval or pupal stages (Fig. S1), yet Wnt4 alters PCP orientation, consistent with the model that Wnt4/Wg act directly on Fz/PCP-interactions. The observation that Wnt4 requires Fz to affect neighboring cells (Fig. 2d–e) further supports this model. It is likely that besides the Wg/Wnt4 input and mechanism identified here, both early and late PCP axes depend on additional cues, provided for instance by the parallel Ft/Ds-PCP system or other morphogenetic organizers[20,21,31,54,55]. Strikingly, such a scenario would suggest that Wg regulates PCP directionality through both PCP systems, affecting Fz/PCP interactions directly (this study) and through canonical Wg-signaling transcriptionally regulating graded *fj* and *ds* expression in eyes and wings[46,55,56]. In summary, our data provide insight into Wnt-mediated mechanisms to directly regulate long-range Fz/PCP orientation by modulating Fz-Vang/PCP interactions during tissue morphogenesis.

Supplementary Material

Refer to Web version on PubMed Central for supplementary material.

Acknowledgements

References

1. Adler PN. Planar signaling and morphogenesis in *Drosophila*. Developmental Cell. 2002; 2:525–535. [PubMed: 12015961]

2. Zallen JA. Planar polarity and tissue morphogenesis. Cell. 2007; 129:1051–1063. [PubMed: 17574020]

3. Seifert JR, Mlodzik M. Frizzled/PCP signalling: a conserved mechanism regulating cell polarity and directed motility. Nature Reviews Genetics. 2007; 8:126–138.

4. Goodrich LV, Strutt D. Principles of planar polarity in animal development. Development. 2011; 138:1877–1892. [PubMed: 21521735]

5. Wu J, Mlodzik M. A quest for the mechanism regulating global planar cell polarity of tissues. Trends in Cell Biology. 2009; 19:295–305. [PubMed: 19560358]

6. Wang Y, Nathans J. Tissue/planar cell polarity in vertebrates: new insights and new questions. Development. 2007; 134:647–658. [PubMed: 17259302]

7. Simons M, Mlodzik M. Planar cell polarity signaling: from fly development to human disease. Annual Reviews of Genetics. 2008; 42:517–540.

8. Wallingford JB. Planar cell polarity, ciliogenesis and neural tube defects. Human Molecular Genetics. 2006; 15(Spec No 2):R227–234. [PubMed: 16987888]

9. Adler PN, Krasnow RE, Liu J. Tissue polarity points from cells that have higher Frizzled levels towards cells that have lower Frizzled levels. Curr Biol. 1997; 7:940–949. [PubMed: 9382848]

10. Jones KH, Liu J, Adler PN. Molecular analysis of EMS-induced *frizzled* mutations in *Drosophila melanogaster*. Genetics. 1996; 142:205–215. [PubMed: 8770598]

11. Wu J, Mlodzik M. The frizzled extracellular domain is a ligand for Van Gogh/Stbm during nonautonomous planar cell polarity signaling. Developmental Cell. 2008; 15:462–469. [PubMed: 18804440]

12. Usui T, et al. Flamingo, a seven-pass transmembrane cadherin, regulates planar cell polarity under the control of Frizzled. Cell. 1999; 98(5):585–595. [PubMed: 10490098]

13. Chen WS, et al. Asymmetric homotypic interactions of the atypical cadherin flamingo mediate intercellular polarity signaling. Cell. 2008; 133:1093–1105. [PubMed: 18555784]

14. Devenport D, Fuchs E. Planar polarization in embryonic epidermis orchestrates global asymmetric morphogenesis of hair follicles. Nature Cell Biology. 2008; 10:1257–1268. [PubMed: 18849982]

15. Strutt H, Strutt D. Differential Stability of Flamingo Protein Complexes Underlies the Establishment of Planar Polarity. Curr Biol. 2008; 18:1555–1564. [PubMed: 18804371]

16. Lawrence PA, Struhl G, Casal J. Planar cell polarity: A bridge too far? Curr Biol. 2008; 18:R959–961. [PubMed: 18957252]

17. Struhl G, Casal J, Lawrence PA. Dissecting the molecular bridges that mediate the function of Frizzled in planar cell polarity. Development. 2012; 139:3665–3674. [PubMed: 22949620]

18. Klein TJ, Mlodzik M. PLANAR CELL POLARIZATION: An Emerging Model Points in the Right Direction. Annual Rev. of Cell and Dev Biol. 2005; 21:155–176. [PubMed: 16212491]

19. Amonlirdviman K, et al. Mathematical modeling of planar cell polarity to understand domineering nonautonomy. Science. 2005; 307:423–426. [PubMed: 15662015]

20. Casal J, Lawrence PA, Struhl G. Two separate molecular systems, Dachsous/Fat and Starry night/Frizzled, act independently to confer planar cell polarity. Development. 2006; 133:4561–4572. [PubMed: 17075008]

21. Lawrence PA, Struhl G, Casal J. Planar cell polarity: one or two pathways? Nature Reviews Genetics. 2007; 8:555–563.

22. Rogulja D, Rauskolb C, Irvine KD. Morphogen control of wing growth through the Fat signaling pathway. Developmental Cell. 2008; 15:309–321. [PubMed: 18694569]

23. Donoughe S, DiNardo S. dachsous and frizzled contribute separately to planar polarity in the Drosophila ventral epidermis. Development. 2011; 138:2751–2759. [PubMed: 21613320]

24. Lawrence PA, Casal J, Struhl G. Cell interactions and planar polarity in the abdominal epidermis of Drosophila. Development. 2004; 131:4651–4664. [PubMed: 15329345]

25. Tada M, Smith JC. Xwnt11 is a target of *Xenopus* Brachyury: regulation of gastrulation movements via Dishevelled, but not through the canonical Wnt pathway. Development. 2000; 127:2227–2238. [PubMed: 10769246]

26. Heisenberg CP, et al. Silberblick/Wnt11 mediates convergent extension movements during *zebrafish* gastrulation. Nature. 2000; 405:76–81. [PubMed: 10811221]

27. Kilian B, et al. The role of Ppt/Wnt5 in regulating cell shape and movement during *zebrafish* gastrulation. Mech Development. 2003; 120:467–476.

28. Gros J, Serralbo O, Marcelle C. WNT11 acts as a directional cue to organize the elongation of early muscle fibres. Nature. 2009; 457:589–593. [PubMed: 18987628]

29. Gao B, et al. Wnt signaling gradients establish planar cell polarity by inducing Vangl2 phosphorylation through Ror2. Developmental Cell. 2011; 20:163–176. [PubMed: 21316585]

30. Vivancos V, et al. Wnt activity guides facial branchiomotor neuron migration, and involves the PCP pathway and JNK and ROCK kinases. Neural Dev. 2009; 4:7. [PubMed: 19210786]

31. Sagner A, et al. Establishment of Global Patterns of Planar Polarity during Growth of the Drosophila Wing Epithelium. Curr Biol. 2012; 22:1296–1301. [PubMed: 22727699]

32. Lim J, Norga KK, Chen Z, Choi KW. Control of planar cell polarity by interaction of DWnt4 and four-jointed. Genesis. 2005; 42:150–161. [PubMed: 15986451]

33. Sato M, Umetsu D, Murakami S, Yasugi T, Tabata T. DWnt4 regulates the dorsoventral specificity of retinal projections in the Drosophila melanogaster visual system. Nature Neuroscience. 2006; 9:67–75. [PubMed: 16369482]

34. Couso JP, Bate M, Martinez-Arias A. A wingless-dependent polar coordinate system in Drosophila imaginal discs. Science. 1993; 259:484–489. [PubMed: 8424170]

35. Gieseler K, et al. DWnt4 and wingless elicit similar cellular responses during imaginal development. Developmental Biology. 2001; 232:339–350. [PubMed: 11401396]

36. Janson K, Cohen ED, Wilder EL. Expression of DWnt6, DWnt10, and DFz4 during Drosophila development. Mech Development. 2001; 103:117–120.

37. Aigouy B, et al. Cell flow reorients the axis of planar polarity in the wing epithelium of Drosophila. Cell. 2010; 142:773–786. [PubMed: 20813263]

38. Strutt H, Warrington SJ, Strutt D. Dynamics of core planar polarity protein turnover and stable assembly into discrete membrane subdomains. Developmental Cell. 2011; 20:511–525. [PubMed: 21497763]

39. Zheng L, Zhang J, Carthew RW. *frizzled* regulates mirror-symmetric pattern formation in the *Drosophila* eye. Development. 1995; 121(9):3045–3055. [PubMed: 7555730]

40. Ng M, Diaz-Benjumea FJ, Vincent JP, Wu J, Cohen SM. Specification of the wing by localized expression of wingless protein. Nature. 1996; 381:316–318. [PubMed: 8692268]

41. Strutt H, Strutt D. Nonautonomous planar polarity patterning in *Drosophila*: *dishevelled*-independent functions of *frizzled*. Developmental Cell. 2002; 3:851–863. [PubMed: 12479810]

42. Couso JP, Bishop SA, Martinez Arias A. The wingless signalling pathway and the patterning of the wing margin in *Drosophila*. Development. 1994; 120:621–636. [PubMed: 8162860]

43. Blair SS. A role for the segment polarity gene shaggy-zeste white 3 in the specification of regional identity in the developing wing of Drosophila. Dev Biology. 1994; 162:229–244.

44. Brand AH, Perrimon N. Targeted gene expression as a means of altering cell fates and generating dominant phenotypes. Development. 1993; 118:401–415. [PubMed: 8223268]

45. Lawrence PA, Casal J, Struhl G. Towards a model of the organisation of planar polarity and pattern in the Drosophila abdomen. Development. 2002; 129:2749–2760. [PubMed: 12015301]

46. Cho E, Irvine KD. Action of fat, four-jointed, dachsous and dachs in distal-to-proximal wing signaling. Development. 2004; 131:4489–4500. [PubMed: 15342474]

47. Neumann CJ, Cohen SM. Long-range action of Wingless organizes the dorsal ventral axis of the Drosophila wing. Development. 1997; 124:871–880. [PubMed: 9043068]

48. Zecca M, Basler K, Struhl G. Direct and long-range action of a wingless morphogen gradient. Cell. 1996; 87:833–844. [PubMed: 8945511]

49. Buratovich MA, Phillips RG, Whittle JR. Genetic relationships between the mutations spade and Sternopleural and the wingless gene in Drosophila development. Developmental Biology. 1997; 185:244–260. [PubMed: 9187086]

50. Cadigan KM, Fish MP, Rulifson EJ, Nusse R. Wingless repression of *Drosophila frizzled 2* expression shapes the Wingless morphogen gradient in the wing. Cell. 1998; 93:767–777. [PubMed: 9630221]

51. Wu CH, Nusse R. Ligand receptor interactions in the Wnt signaling pathway in Drosophila. Journal of Biol Chemistry. 2002; 277:41762–41769.

52. Chen CM, Strapps W, Tomlinson A, Struhl G. Evidence that the cysteine-rich domain of Drosophila Frizzled family receptors is dispensable for transducing Wingless. Proceedings of the National Academy of Sciences (USA). 2004; 101:15961–15966.

53. Gubb D, Garcia-Bellido A. A genetic analysis of the determination of cuticular polarity during development in Drosophila melanogaster. J Embryol Exp Morphol. 1982; 68:37–57. [PubMed: 6809878]

54. Ma D, Yang CH, McNeill H, Simon MA, Axelrod JD. Fidelity in planar cell polarity signalling. Nature. 2003; 421:543–547. [PubMed: 12540853]

55. Yang CH, Axelrod JD, Simon MA. Regulation of Frizzled by fat-like cadherins during planar polarity signaling in the *Drosophila* compound eye. Cell. 2002; 108(5):675–688. [PubMed: 11893338]

56. Zecca M, Struhl G. A feed-forward circuit linking wingless, fat-dachsous signaling, and the warts-hippo pathway to Drosophila wing growth. PLoS Biol. 8:e1000386. [PubMed: 20532238]

57. Lawrence PA, Johnston P, Vincent JP. Wingless can bring about a mesoderm-to ectoderm induction in Drosophila embryos. Development. 1994; 120:3355–3359. [PubMed: 7821207]

58. Boutros M, Mihaly J, Bouwmeester T, Mlodzik M. Signaling specificity by Frizzled receptors in *Drosophila*. Science. 2000; 288:1825–1828. [PubMed: 10846164]

59. Cohen ED, et al. DWnt4 regulates cell movement and focal adhesion kinase during Drosophila ovarian morphogenesis. Developmental Cell. 2002; 2:437–448. [PubMed: 11970894]

60. van den Heuvel M, Harryman-Samos C, Klingensmith J, Perrimon N, Nusse R. Mutations in the segment polarity genes wingless and porcupine impair secretion of the wingless protein. EMBO J. 1993; 12:5293–5302. [PubMed: 8262072]

61. Tiong SY, Nash D. Genetic analysis of the adenosine3 (Gart) region of the second chromosome of Drosophila melanogaster. Genetics. 1990; 124:889–897. [PubMed: 2108904]

62. Brook WJ, Cohen SM. Antagonistic interactions between wingless and decapentaplegic responsible for dorsal-ventral pattern in the Drosophila Leg. Science. 1996; 273:1373–1377. [PubMed: 8703069]

63. Bhat MA, et al. Discs Lost, a novel multi-PDZ domain protein, establishes and maintains epithelial polarity. Cell. 1999; 96:833–845. [PubMed: 10102271]

64. Wu J, Cohen SM. Proximal distal axis formation in the Drosophila leg: distinct functions of teashirt and homothorax in the proximal leg. Mech Development. 2000; 94:47–56.

65. Oda H, Uemura T, Harada Y, Iwai Y, Takeichi M. A *Drosophila* homolog of cadherin associated with armadillo and essential for embryonic cell-cell adhesion. Developmental Biology. 1994; 165:716–726. [PubMed: 7958432]

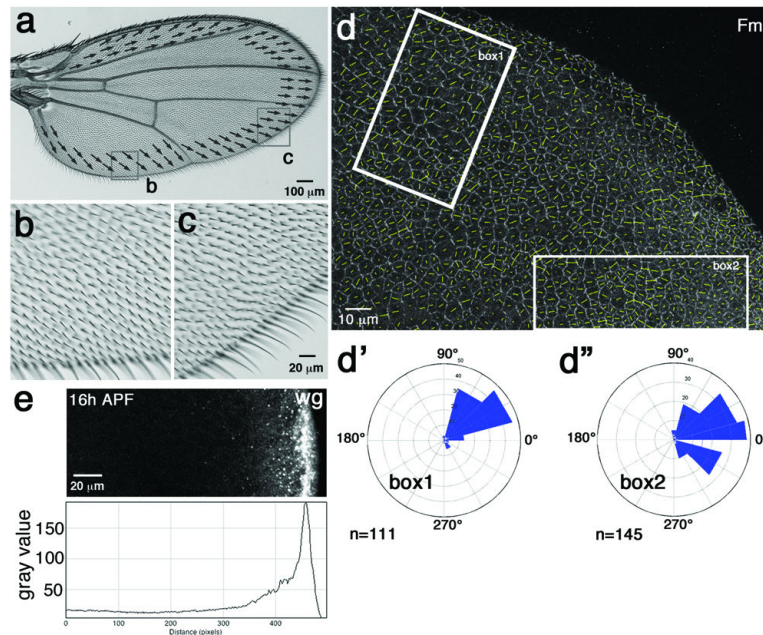**Figure 1. Wg/Wnt expression and planar cell polarity patterning**
(**a-a'**) Wild-type wing with semi-schematic illustration of cell orientation/wing hair direction in areas near wing margin. (**b**–**c**) High magnification views of boxed areas from panel **a**, demonstrating orientation towards wing margin. (**d-d''**) Wild-type 16h APF (after puparium formation) pupal wing stained for anti-Fmi, reflecting cellular orientation (as quantified[37]; highlighted by yellow lines in each cell; vector length indicates nematic order/polarity strength). Fmi polarization in box 1 region points towards margin (about 45° away from proximal distal axis; quantified in d'), see also equivalent radial polarization for Vang-GFP[37]. Fmi polarization in box 2 region is also oriented radially towards the margin (quantif. in **d''**; *n*=number of cells in indicated area; all wild-type wings at this stage show the same PCP features, 5 were analyzed in detail. (**e**) Wg is expressed in all wing margin cells and forms a gradient away from the margin at all stages. Example shown is from 16h APF pupal wing.
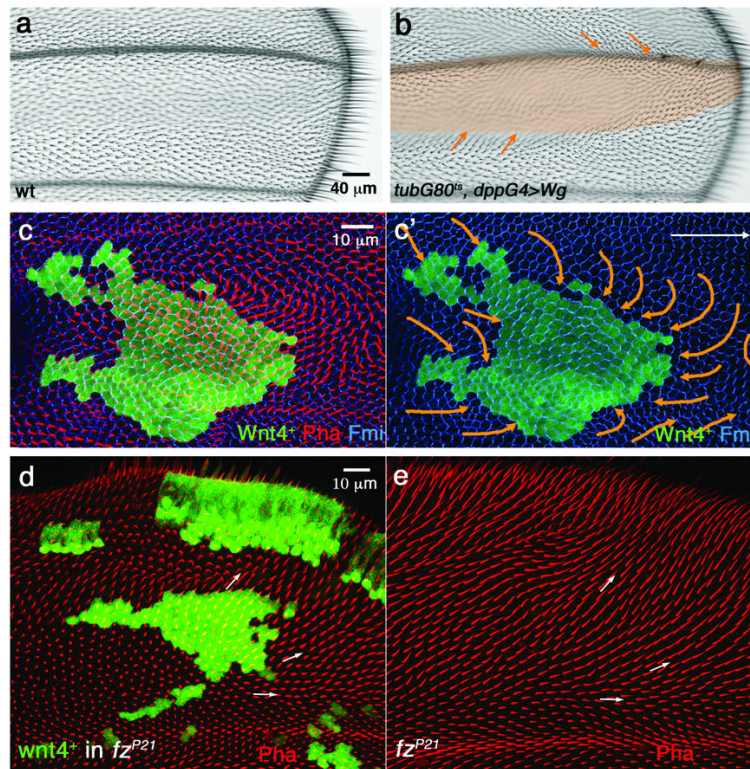
Figure 2. Ectopic dWnt4 or Wg expression reorients PCP direction in neighboring cells
(**a**) Wild-type wing with hairs pointing distally. (**b**) *tubGal80^{ts}*/*Gal4* system with *dppGal4*
driver is used to express Wg ectopically (0–1h APF pupae were aged at 18°C for 12 hours
(about 6 hours APF at 25°), then shifted from 18°C to 29°C for 8 hours to induce Wg
expression before shifting back to 18°C). Note that cell orientation (visible by their cellular
hairs) outside the expression domain reorients towards the Wg-misexpression domain
(highlighted by orange shading). Distal is to the right and anterior up in all panels. (**c-c'**)
Ectopic Wnt4 expression clone (marked by co-expression of GFP, green) analyzed in 32h
APF pupal wings with anti-Fmi (blue) and Phalloidin (actin, red). Cells surrounding the
clone reorient their polarity towards the clone, visible both by growing actin hairs (red in **c**)
and axis of Fmi polarization (**c'**, orange arrows illustrate the underlying polarity of the
respective cellular fields). 36 Wnt4 GOF clones were analyzed by Fmi staining, 5 at early
(15–16h APF) stage and 31 at later stages (30–31h APF); approx. 72% displayed
phenotypes as presented here and in Figs. 3 and 4. (**d**) Wnt4 expressing clones (marked by
co-expression of GFP-green) in *fz^{P21/P21}* pupal wing (lacking *fz* in the entire wing) at 32–
33h APF. (**e**) Wing of same genotype as in (**d**), but lacking ectopic Wnt4-expression
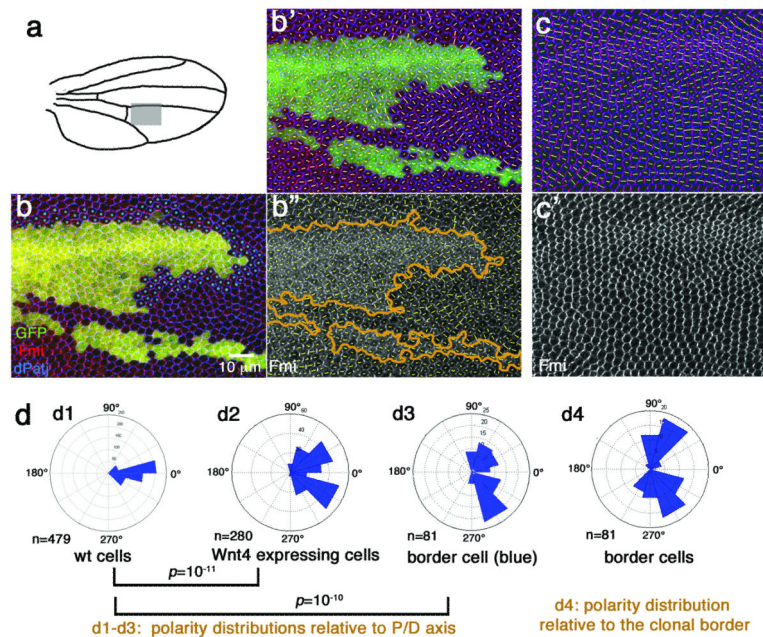(serving as *fz^{P21/P21}* control).

Figure 3. Ectopic Wnt4 expression reorients Fz/PCP factors in pupal wings

(**a**) Schematic illustration of wing. Grey box indicates region containing Wnt4 expressing clone in panels **b-b"** and wild-type control in **c**. (**b-b"**) Wnt4 expressing clone (labeled by GFP expression, green) induced during early second instar. 0–1h APF white pupae were aged for 27h at 29°C (about 31h APF at 25°C, just prior to wing hair formation). Fmi (red, monochrome in **b"**) detects PCP orientation and dPatj (blue) outlines all cells. Polarity of individual cells (Fmi localization) was plotted as yellow lines, calculated/quantified as described[37] (**b'-b"**). Blue dots indicate 2–3 rows of border cells neighboring the clone. (**c-c'**) wild-type control wing imaged in same region with same markers.

(**d**) Rosettes presenting cellular orientation angles (*n*=number of cells; 36 Wnt4 GOF clones were analyzed by Fmi staining, 31 at this stage [approx. 30h APF] and 5 at early stages [15–16h APF], approx. 72% displayed phenotypes as presented here and in Fig. 4): **d1**, wild-type with general P–D axis orientation; **d2**, Wnt4+ cells (note randomized angle distribution; $p=10^{-11}$ as calculated with two-sample Kolmogorov-Smirnov test comparing the patterns in d1 with d2 in the same area of independent pupal wings; see Methods for details on statistical analyses); **d3**, polarity angles of cells bordering clone (marked by blue dots in **b**) are different from wild-type ($p=10^{-10}$ with Kolmogorov-Smirnov compared to d1); **d4**, polarity angles relative to clonal borders display angles near 90°/-90°, indicating that cells orient towards clonal borders, as wing hair direction (Fig. 2c) established that polarity points towards clones. Unmarked "border cells" were excluded from the analysis, because these receive ectopic Wnt4 from multiple directions [e.g. the small clone at bottom which was not analyzed here]).
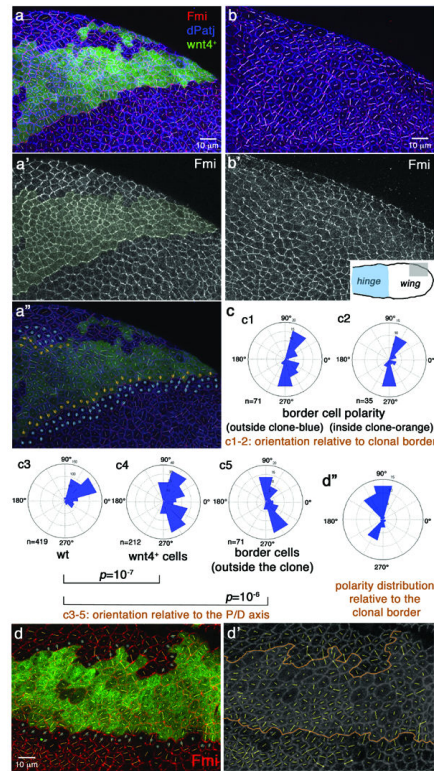
Figure 4. Wnt4 misexpression reorients PCP during early pupal development

Panels show 16h APF pupal wings with Wnt4 misexpression clones (**a-a''** and **d-d'**; marked by GFP, green; yellow shading in **a'**). **b-b'**: wild-type control for direct comparison. Inset in **b'** illustrates area displayed in **a–b** (hinge region marked blue). Anti-Fmi (red in multicolor panels, monochrome in **a',b'**) and anti-dPatj (blue in **a,a'',b**) reflect cellular orientation (Fmi) and cell outlines (dPatj). Polarization (Fmi localization) was calculated/quantified as described[37], illustrated as white or yellow lines in each cell: orientation of lines indicates polarity direction, length indicates strength of polarization/nematic order (see below). (**a''**) Cells bordering Wnt4 source, on inside and outside of clone, are highlighted with orange and blue dots, respectively; see (**c**) for orientation angles.

(**c**) Polarization of specific cell populations from (**a–b**) as labeled. **c1, c2**: polarity relative to clonal border; **c3–c5**: actual polarity as present in wing area (*n*=number of cells scored/ rosette; 36 Wnt4 GOF clones were analyzed by Fmi staining, 5 independent wings were analyzed at this stage [15–16h APF] and 31 at later stages [see also Fig. 3]). Wnt4-misexpression affects cellular polarization autonomously (polarity distribution of Wnt4+ cells [**c4**] is different from wild-type [**c3**]; $p=10^{-7}$ with two-sample Kolmogorov-Smirnov, see Methods) and non-autonomously: polarity of neighboring cells (2–3 rows marked by blue dots in [**a''**]) are distinct from wild-type in same region (**c3** vs **c5**; $p=10^{-6}$ with Kolmogorov-Smirnov) and near 90°/-90° relative to clonal borders (**c1**). Border cells inside clone (orange dots in **a''**) are also near 90° relative to clonal border (compare **c2** and **c1**) and distinct from wild-type ($p=10^{-5}$).

(**d-d''**) Different example of Wnt4+ clone at same stage. Note random polarity in clone and near 90°/-90° orientation of border cells relative to clonal border (blue dots in **d**; rosette in

d"). 4/5 Wnt4 expressing clones analyzed at 15–17h APF altered Fmi polarization in neighboring cells.Nematic order, represented by length of polarity lines in each cell (see **a– b**) is affected by Wnt-expressing clones. Wnt4+ cells have reduced polarity vs non-wnt4 expressing (wild-type) cells (59.8+/−13.2 vs 72.1+/−15.8; *p*=0.005 with student *t*-test; average nematic order +/−standard deviation are shown), whereas border cells (blue/orange dots in a") are more polarized (compared to Wnt4+ cells: 78.4+/−15.2 vs. 59.8+/−13.2; *p*=0.004; average nematic order +/−standard deviation; *n*=number of cells; 5 independent wings were scored).
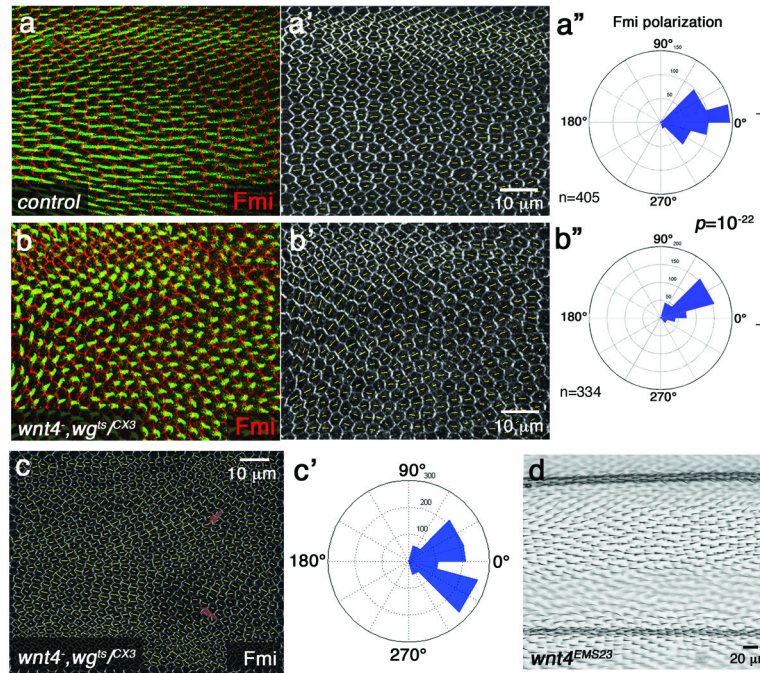
Figure 5. *dWnt4, wg* double mutant loss-of-function wings display PCP defects

Panels **a–c** show pupal wings; panel **d** an adult wing; anterior is up and distal to the right. (**a-a"**) wg^{CX3}/wg^{IL114} (single mutant) pupal wing, shifted from 16.5° to 29°C at 0–1h APF and incubated for 29 hours prior to dissection. Fmi (red; monochrome in **a'**) and Phalloidin (green, displaying actin prehairs) staining is shown. Most such wings display a normal PCP appearance comparable to wild-type. Cellular polarity (and nematic order), as highlighted by Fmi staining, was calculated according to[37] and plotted as yellow lines. For respective polarity distribution see **a"** (*n*=number of cells; 5 wings were analyzed). (**b-b"**) $wnt4^{-/-}$, $wg^{CX3/ts}$ double mutant pupal wing, shifted and stained as in **a** (also same wing region as in [**a**]). PCP defects are evident by mispolarized Fmi staining/polarity orientation (red; monochrome in **b'**) and wing hair orientation (Phalloidin, green). Cellular polarity (yellow lines in **b'**) was calculated as in **a'** and resulting polarity distribution is shown in **b"** (*n*=number of cells; 5 wings were analyzed). It is distinct from control (**a-a'**) wing in the same area ($p=10^{-22}$ with two-sample Kolmogorov-Smirnov, see Methods). 9/10 $wnt4^{-/-}$, $wg^{CX3/ts}$ double mutant wings show such Fmi localization PCP defects, whereas $wnt4^-$ ($wnt4^{EMS23}$) wings did not show PCP defects (**d**). (**c-c'**) An additional example of a $wnt4^{-/-}$, $wg^{CX3/ts}$ double mutant pupal wing for comparison.
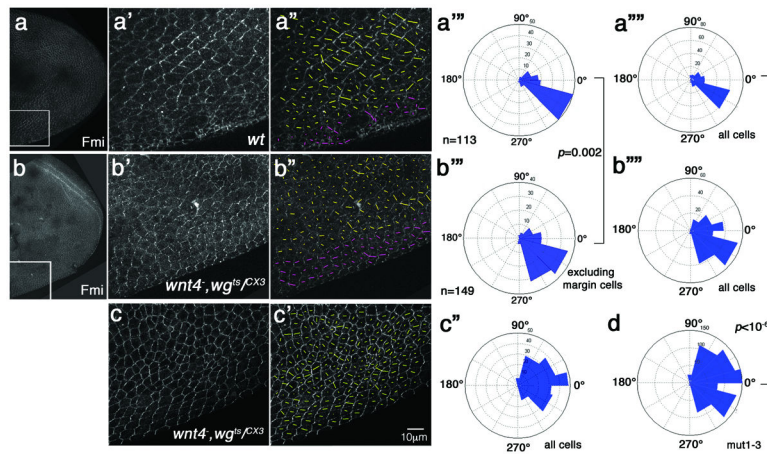
Fig. 6. *dWnt4, wg* double mutants display early loss of PCP orientation

All panels show 16h APF pupal wings (anterior is up and distal to the right), with the respective polarity distributions in rosette diagrams. (**a-a''''**) wild-type, and (**b–c''''**) *wnt4*$^{-/-}$, *wg*$^{CX3/ts}$ double mutant pupal wings shifted at 0–1h APF to 29°C and incubated for 15 hours (about 16h APF at 25°C). (**a',b'**) display high magnification view of boxed areas in (**a**) and (**b**). (**c**) Same pupal wing area of an independent *wnt4*$^{-/-}$, *wg*$^{CX3/ts}$ double mutant. Fmi staining (monochrome) was used as PCP orientation marker and polarity and strength/nematic order were plotted as yellow lines (**a''**, **b''** and **c'**). Cells close to wing margin are less (or not) polarized as previously reported[37] (the 3 margin proximal rows highlighted by pink lines were excluded from polarity analysis in rosette diagrams in **a'''** and **b'''**, for comparison; all other rosette diagrams include all cells. (**d**) shows the sum of three independent *wnt4*$^{-}$, *wg*$^{CX3/ts}$ mutant wings. *wnt4*$^{-}$, *wg*$^{CX3/ts}$ double mutant wings showed much wider polarity distribution than wild-type (compare **a'''** with **b'''** [*p*=0.002 with two-sample Kolmogorov-Smirnov test, *n*=number of cells]; or **a''''** with **b''''** and **d**; *p*<10^{-6}; 3/3 *wnt4*$^{-/-}$, *wg*$^{CX3/ts}$ wing discs quantified displayed very similar phenotypes; 2 examples shown in **b** and **c** panels, **d** shows sum of all three). Overall polarization/nematic order level was markedly reduced from wild-type to the *wnt4*$^{-}$, *wg*$^{CX3/ts}$ double mutants (wt: 59.13+/−36.65 vs mutant: 35.68+/− 20.00 *p*=10^{-26} with *t*-test; average nematic order +/− s.d.). All double mutant wings analyzed show complete lack of orientation and reduced overall polarization (3 out of 3 quantified *wnt4*$^{-/-}$, *wg*$^{CX3/ts}$ and all others not quantified in detail displayed visually very similar phenotypes).
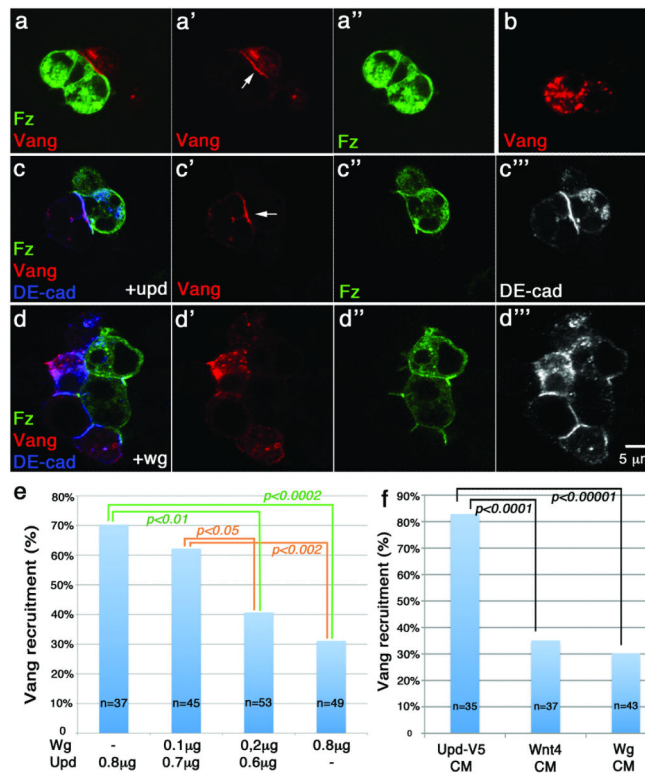
Figure 7. Wg/Wnt4 inhibit intercellular Fz recruitment of Vang to the cell membrane

(**a-a''**) S2+R cells co-transfected with Fz-YFP (green) and DE-cadherin were mixed with S2+R cells co-transfected with Vang-Flag (red) and DE-cad. Vang (red) is recruited to cell membrane (arrow) in areas that are in contact with neighboring Fz expressing cells. Anti-GFP and anti-Flag were used to detect Fz-YFP and Vang-Flag proteins, respectively.

(**b**) Vang-Flag, E-cad transfected cells alone (not mixed with Fz transfected cells), display Vang protein in vesicular structures, but not at the membrane.

(**c-c'''**) S2+R cells co-transfected with Fz-YFP (green), DE-cad (blue), and Unpaired (Upd) were mixed with S2+ cells co-transfected with Vang-Flag (red) and DE-cad (blue). Upd was used as a control secreted ligand; it did not affect intercellular Vang recruitment by Fz (arrow). Cells in contact expressed DE-cad localized to their contact sites (blue; monochrome in **c'''**).

(**d-d'''**) S2+R cells co-transfected with Fz-YFP (green), DE-cad (blue), and Wg were mixed with S2+ cells co-transfected with Vang-Flag (red) and DE-cad (blue). In the presence of Wg (0.8 μg), Fz largely failed to recruit Vang to the contacting cell membranes. Fz membrane localization was not affected.

(**e**) Quantification of Wg effect on intercellular Fz-Vang recruitment. Increasing amounts of Wg DNA (as indicated) were co-transfected with Fz/DE-cad cells, which were subsequently mixed with Vang/DE-cad transfected cells. Vang recruitment shown as % of total cell pairs analyzed (*n*=number of contacting pairs; 3 independent experiments were used to score these). Statistical analysis: Fischer's exact test (two-tailed) and *p* values are as indicated. Inhibitory effect of Wg on Fz-Vang recruitment is dosage dependent and highly reproducible (Suppl. Fig. S4 for additional examples).

(**f**) Secreted extracellular Wnt4 and Wg affect Fz-vang interaction. Conditioned media (CM) with Wnt4 or Wg affect Fz-Vang recruitment, Fz/DE-cad and Vang/DE-cad transfected S2+R cells were incubated in Wnt4, Wg or Upd-V5 (as negative control) CM. Recruitment quantified as percentage of Fz/DE-cad and Vang/DE-cad cell-cell contacts resulting in Vang localization at contact membranes. Vang recruitment was reduced in presence of Wnt4 or Wg CM, *n*=number of contacting cell pairs (statistical analysis as in [**e**]; confirmed by 3 independent experiments; Suppl. Fig. S4 for experimental samples).
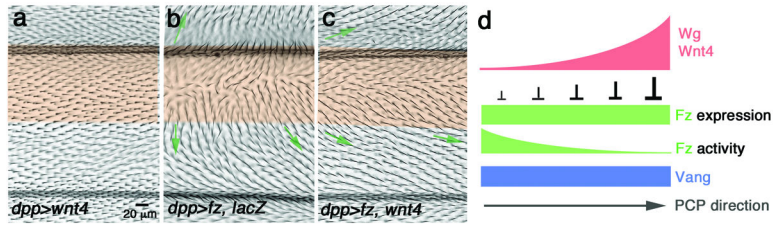
Figure 8. *In vivo* **co-expression of Wnt4 inhibits non-autonomous effects of Fz**
(**a–c**) Adult wings of indicated genotypes, expressing the indicated transgenes under
dppGal4 control (expression domain marked by transparent orange shading); distal is right.
Orientation of neighboring (wild-type) cells is indicated with green arrows. (**a**) *dppGal4,
UAS-Wnt4* alone (this transgene has largely a wild-type appearance), whereas *dppGal4,
UAS-fz* (with *UAS-lacZ/+* as control) causes robust reorientation of neighboring cells (**b;**
aberrant orientation highlighted with green arrows). Co-expression of Fz with Wnt4
(*dppGal4, UAS-fz/UAS-Wnt4*) markedly reduces the non-autonomous effects of Fz (**c**). See
Suppl. Fig.S5 for quantitative and statistical analyses.

(**d**) Model: Schematic illustration of the molecular mechanism involving Wg/dWnt4 in
modulating Fz activity for the Fz-Vang interaction and associated PCP direction
establishment: Wg/Wnt4 binding to Fz generates a "Fz/PCP activity" gradient for the Fz-
Vang interaction. See main text for details and other potential interpretations.